Journal of Chemical Health Risks

www.jchr.org

JCHR (2024) 14(4), 544-560 | ISSN:2251-6727

Exploring the Therapeutic Potential of an Ayurvedic Herbal Formulation Utilizing Trigonella Foenum-Graecum in Diabetes Management: A Comprehensive Study

Tanuja Pawar*, Tejas S. Pachpute

Department of Pharmaceutics, Alwar Pharmacy college, Sunrise University, Alwar, Rajasthan, India

[#] Equal Contribution

*Corresponding author Tanuja Pawar[*]

Email ID: pawartanuja41@gmail.com, tejaspachpute@gmail.com

(**Received**: 14 April 2024 **Revised**: 01 May 2024 **Accepted**: 18 June 2024)

KEYWORDS

Trigonella foenum-graceum, fenugreek, lipid-based nanoparticles, diabetes management, drug delivery

Abstract

This research investigates the development and optimization of a lipid-based nanoparticle (NP) formulation for the delivery of Trigonella foenum-graceum (fenugreek) aimed at diabetes management. Fenugreek, a staple in Ayurvedic medicine, exhibits promising antidiabetic properties, yet its limited solubility hampers its therapeutic efficacy. To address this challenge, lipid-based NPs were engineered to enhance fenugreek's solubility, bioavailability, and therapeutic effectiveness. A systematic formulation approach was adopted, incorporating principles of lipid-based drug delivery systems and nanotechnology. Through statistical tools and experimental design techniques, formulation parameters such as lipid type, surfactant content, and homogenization process were optimized to achieve NPs with desirable characteristics including ideal particle size, high drug loading, and physical stability.

Characterization studies revealed that the lipid-based fenugreek NPs exhibited significantly smaller particle sizes compared to traditional formulations, potentially facilitating improved drug absorption and solubility. Animal model studies underscored the enhanced bioavailability and therapeutic efficacy of the fenugreek NPs, highlighting their potential for diabetes management. However, further investigations encompassing pharmacokinetic and pharmacodynamic assessments are warranted to elucidate their clinical relevance fully.

This study contributes valuable insights into pharmaceutical sciences, showcasing the potential of lipid-based NPs as efficacious drug delivery systems for enhancing the therapeutic effectiveness of poorly soluble natural compounds like fenugreek in diabetes management. The findings open avenues for future research aimed at optimizing and translating these innovative formulations into clinical practice.

1.Introduction

Diabetes mellitus, characterized by elevated blood glucose levels, has emerged as a global health concern with significant implications for morbidity, mortality, and healthcare costs. According to the International Diabetes Federation, approximately 463 million adults were living with diabetes in 2019, with projections indicating a rise to 700 million by 2045. The burden of this metabolic disorder extends beyond its immediate physiological effects, encompassing a spectrum of complications affecting multiple organ systems, including cardiovascular, renal, and neurological [1].

In the quest for effective diabetes management strategies, there is growing interest in traditional systems of medicine that offer holistic approaches to health and wellness. Among these, Ayurveda, the ancient Indian system of medicine, has garnered attention for its emphasis on natural remedies and personalized therapeutic interventions. Central to Ayurvedic philosophy is the concept of balance and harmony within the body, achieved through a combination of dietary modifications, lifestyle practices, and herbal formulations [2].

Trigonella foenum-graceum, commonly known as fenugreek or Methi, occupies a prominent place in Ayurvedic pharmacology for its purported antidiabetic properties. With a rich history of use dating back

Journal of Chemical Health Risks

www.jchr.org

JCHR (2024) 14(4), 544-560 | ISSN:2251-6727

centuries, fenugreek seeds have been employed in various Ayurvedic formulations aimed at managing diabetes and related metabolic disorders. The multifaceted therapeutic potential of fenugreek is attributed to its diverse bioactive constituents, including soluble dietary fibers, saponins, alkaloids, and flavonoids, which exert beneficial effects on glucose metabolism, insulin sensitivity, and pancreatic function [3].

Despite the widespread use of fenugreek in traditional medicine, there remains a paucity of rigorous scientific evidence supporting its efficacy and safety in the context of diabetes management. Consequently, there is a compelling need for well-designed research studies to evaluate the clinical effectiveness of Ayurveda-based herbal formulations incorporating fenugreek as a key ingredient. By bridging the gap between ancient wisdom and modern science, such investigations hold promise for uncovering novel therapeutic options for individuals grappling with the challenges of diabetes [4].

In light of these considerations, this research article aims to explore the potential of an Ayurveda-based herbal formulation of Trigonella foenum-graceum for diabetes management. Through a comprehensive review of existing literature and insights from experimental studies, we endeavor to elucidate the mechanisms of action, pharmacological properties, and clinical implications of this traditional remedy. By advancing our understanding of fenugreek's role in diabetes care, we aspire to contribute to the evolution of integrative approaches to health promotion and disease prevention [5].

2.Material and Method

2.1 Collection of plant material

The collection process for Trigonella Foenum-Graceum, commonly known as fenugreek, was conducted within the expansive botanical garden of MUP's College of Pharmacy in Risod. This plant species was selected due to its well-documented pharmacological properties and rich history of traditional uses. The botanical garden, with its controlled and consistent cultivation conditions, provided an optimal environment for the collection, ensuring the reliability and uniformity of the specimens [6].

2.2 Authentication

Following the meticulous collection of Trigonella Foenum-Graceum, a rigorous authentication process was implemented to verify the accuracy of the obtained plant material from Department of Botany, Sangamner College (Autonomous). This involved comprehensive documentation of key botanical characteristics, growth conditions, and other relevant metadata. Additionally, botanical experts were consulted to visually inspect and confirm the identity of the specimens based on distinctive features such as leaf morphology and flower structure. Furthermore, voucher specimens of the collected plant materials were submitted to the herbarium, establishing a tangible record for future reference and cross-verification. This authentication process not only upholds scientific standards but also ensures that the plant material used in subsequent analyses is indeed Trigonella Foenum-Graceum, laying the groundwork for reliable and credible research [7].

2.3 Microscopical evaluation-powder microscopy

Shade dry TFG leaves. Pass leaf powder through a 60-no. mesh size. Store powders in airtight glass bottles. Maintain 34°C average temperature and 50% humidity during drying. Disperse powders on glass slides. View powders under microscope at various magnifications. Stain powder with phloroglucinol and hydrochloric acid. Stain powder with strong hydrochloric acid, 1% phloroglucinol, and 90% ethanol. Examine stained powder under a microscope. Identify pink-colored lignified tissues (sclereids, xylem vessels, etc.) [8].

2.4 Extraction of TFG leaves

2.4.1 Soxhlet extraction method

To prevent the heat deterioration of the target chemical, the extractions were carried out under lower pressure. Using a solvent ethanol, the extractions were conducted over a six-hour period. The polar portion was obtained by extracting the residual cake with ethanol. All fractions were vacuum-concentrated, then HPLC was used to analyze them. The following equation was used to determine the extraction yields:

$$Yield\left(\%\frac{w}{w}\right) = \frac{Mass\ dried\ extract\ (gm)}{Mass\ dried\ matrix\ (gm)} \times 100$$

2.4.2 Preliminary phytochemical investigation of extract

Thin layer chromatography (TLC):

To separate active chemicals using the thin layer chromatography (TLC) technique. To make the slurry,

Journal of Chemical Health Risks

www.jchr.org

JCHR (2024) 14(4), 544-560 | ISSN:2251-6727

30gm of silica gel G was combined with 100ml of water. A glass plate was filled with the slurry, which was then evenly dispersed across its surface. The glass plates were dried in a hot air oven at 110ºC for an hour after settling. The TLC plate was created with a baseline. The sample was placed in a small area of solution that was put to a plate and dried. Pouring methanol: chloroform (1:9), a suitable solvent (eluent) that exhibits improved compound separation, to a depth of less than 1 cm in a TLC chamber [9].

The container was covered with a lid or cover glass, and saturation was allowed to occur for 10 minutes. The TLC plate was then put in the chamber and the chromatogram is allowed to run. The sample was eluted when the solvent, which was being carried up the plate by capillary action, comes into contact with the sample mixture. The dry plate was put in a chamber with a few iodine crystals. The compounds in the different spots were oxidized by the iodine vapour inside the chamber, made them visible to the human eye. Before the iodine coloration disappears, the dots were highlighted with a pencil once they are visible [10].

Combine 30g of silica gel G with 100ml of water to create a slurry. Fill a glass plate with the slurry and ensure it is evenly dispersed across the entire surface. Place the glass plate in a hot air oven at 110°C for one hour to dry the slurry and allow it to settle. Establish a baseline on the TLC plate using a pencil or marker. Place a small area of the sample solution onto the TLC plate and allow it to dry. Pour a suitable solvent (eluent) such as methanol: chloroform (1:9) into the TLC chamber to a depth of less than 1cm. Cover the TLC chamber with a lid or cover glass and let it saturate for 10 minutes. Place the TLC plate into the chamber and allow the chromatogram to develop [11].

The capillary action will move the solvent up the plate. When the sample combination comes into touch with the solvent that is travelling along the plate, it will be eluted. Placing the dry plate inside a chamber with a few iodine crystals will help. The chemicals will oxidise inside the chamber and become apparent to the naked eye. Use a pencil to highlight the spots after they become noticeable because of the iodine coloration before the coloration fades. Utilising the solute's travel distance to the solvent, calculate Rf [12].

$$Rf\ value = \frac{Distance\ Travelled\ by\ the\ solute}{Distance\ travelled\ by\ the\ solvent}$$

High-Performance Thin Layer Chromatography (HPTLC):

An appropriate mobile phase was essential for optimizing the HPTLC process and creating a stability-indicating assay technique. A solution of 50% v/v methanol was created to prepare the mobile phase. A 10 ml volumetric flask was filled with TFG drug powder that had been precisely weighed. The contents were thoroughly dissolved using a sonicator and 5 ml of 50% Methanol. With 50% Methanol, the volume was then brought to 10 ml. The solution was sonicated for an additional ten minutes before being filtered using Whatman filter paper. This filtered solution was utilized for HPTLC analysis and kept in 5 ml glass vials. The plates were produced in a twin trough chamber in saturated mode at room temperature, dried thereafter, and then subjected to densitometry scanning. The CAMAG TLC scanner 4 was then used to scan the HPTLC plate at a wavelength of 270 nm. The CAMAG win CATS computer programme was used to display the generated densitogram. By contrasting the Rf values and area under the curve values obtained for the sample with those obtained for a standard, analysis and validation were carried out [13].

2.5 Formulation and Development

Lyophilization of extract in freeze dryer (Benchtop):

The NPs underwent freeze-thaw tests to assess how different lyoprotectants behaved before being lyophilized. 1 mL of each sample was cooled to 5ºC from room temperature in the freezing step at a rate of 5ºC/minute, followed by a 15ºC isothermal incubation. The NPs were then frozen to -55ºC at a rate of 1ºC/minute and maintained at this temperature for a minimum of 60 minutes. The formulations were heated to 5ºC at a rate of 1ºC/minute to thaw them. The trials made use of three duplicates of each formulation [14].

The VirTis Advantage Plus Benchtop lyophilizer offers a convenient and efficient method for the freeze drying (lyophilization) of NPs. Prepare the nanoparticle suspension by dispersing the NPs in a suitable solvent or buffer. Ensure that the suspension is well-mixed and free from any aggregates or impurities. Transfer the suspension into vials or containers that are compatible with the lyophilizer ensuring a maximal height of 10 mm. Next, place the vials or containers into the lyophilizer chamber, making sure they are properly arranged and secured to prevent any leakage. Close the chamber door

Journal of Chemical Health Risks

www.jchr.org

JCHR (2024) 14(4), 544-560 | ISSN:2251-6727

and initiate the lyophilization cycle. The VirTis Advantage Plus Benchtop lyophilizer offers user-friendly control panels, allowing you to set the desired parameters such as temperature, pressure, and drying time [15].

Once the lyophilization cycle begins, the system will gradually lower the temperature to initiate freezing of the nanoparticle suspension at -55ºC for 5 hours. The freezing process converts the liquid phase into a solid phase, preserving the NPs. After freezing, the system will gradually reduce the chamber pressure, creating a vacuum environment. This was followed by a primary drying step at -45ºC and a pressure of 400 mTorr for 40 hours [16].

In the subsequent sublimation step, the frozen solvent in the nanoparticle suspension will transition directly from the solid phase to the gas phase, bypassing the liquid phase. This sublimation process removes the solvent, leaving behind the freeze-dried NPs. Throughout this stage, the lyophilizer continuously monitors and controls the temperature, pressure, and drying time to ensure optimal results. Once the desired drying time has elapsed, the lyophilization cycle is complete. Open the chamber door and carefully remove the vials or containers containing the freeze-dried NPs. It is important to handle the samples in a controlled environment to avoid moisture uptake [17].

Finally, store the freeze-dried NPs in appropriate containers, such as sealed vials, to protect them from moisture and other environmental factors. These dried NPs can be reconstituted using a suitable solvent or buffer before further characterization or application. The VirTis Advantage Plus Benchtop lyophilizer provides a reliable and efficient method for the freeze drying of NPs. The system offers precise control over temperature, pressure, and drying time, allowing for the preservation of nanoparticle integrity during the lyophilization process [18].

Preparation of polymeric-NPs (Solvent Evaporation method):

The solvent evaporation method is a widely used technique for the preparation of polymeric NPs, which involves the formation of an oil-in-water emulsion followed by solvent evaporation. The step-by-step procedure for preparing polymeric NPs using chitosan, lyophilized extract and methanol as excipients was as follows: Firstly, an organic phase was prepared by dissolving chitosan in methanol. The chitosan should be accurately weighed and added to a suitable container. An appropriate amount of methanol was then poured into the container, and the mixture was stirred using a magnetic stirrer or vortex mixer until the chitosan was completely dissolved, ensuring a homogeneous solution was obtained. Next, the drug solution was prepared by dissolving the active ingredient or drug in a suitable solvent, such as water or ethanol. Additional solvents may be required depending on the solubility of the drug. The drug solution thoroughly mixed to ensure proper dissolution or dispersion of the drug. Nanoparticle formation occurred by slowly adding the drug solution to the chitosan-methanol solution while continuously stirring. This addition was done dropwise to prevent rapid mixing and allow for the formation of NPs. Care was taken to control the rate of addition to ensure proper encapsulation of the drug within the NPs [19].

After the drug solution was added, the mixture was further stirred for a specific period of time to promote nanoparticle formation. The solution was then transferred to a suitable device such as a rotary evaporator, where the methanol solvent was evaporated. The evaporation process conducted under controlled conditions, such as reduced pressure and gentle heating, to facilitate the removal of methanol and promote the formation of solidified NPs. Once the solvent has completely evaporated, the polymeric NPs were formed. NPs can be collected by centrifugation or filtration using a suitable membrane or filter paper. The collected NPs were then washed with a suitable solvent, such as water or ethanol, to remove any residual excipients or unencapsulated drug. The obtained polymeric NPs should be characterized for size, size distribution, morphology, and drug loading efficiency using techniques like dynamic light scattering, scanning electron microscopy, and UV-Vis spectroscopy. The NPs stored in a suitable container under appropriate conditions, such as refrigeration or freeze-drying, to maintain their stability for long-term storage and further use [20].

The different NPs of TFG NP-1, NP-2, NP-3 and NP-4 containing molar ratio of chitosan and TFG extract were prepared as mentioned in Table 1.

Journal of Chemical Health Risks

www.jchr.org

JCHR (2024) 14(4), 544-560 | ISSN:2251-6727

Table 1: Different formulation of NPs containing molar ratio of chitosan and TFG extract.

NPs batch	Molar ratio Chitosan (mg): Extract(mg)	Methanol
NP-1	0.5: 1	20mL
NP-2	1:1	20mL
NP-3	2:1.5	20mL
NP-4	3:2	20mL

2.6 Evaluation of batches

2.6.1 Entrapment efficiency

The efficiency of the formulations for drug entrapment was assessed by centrifuging the aqueous solution. The quantity of the free drug was found in the supernatant, and the amount of the drug that had been integrated was calculated by subtracting the amount of the free drug from the original drug. At 233 nm, entrapment efficiency, a measure of the amount of drug incorporated, was calculated spectrophotometrically [66]. The following formula was used to determine the entrapment efficiency [21].

$$\%\ Entrapment\ efficiency = \frac{(Weight\ of\ initial\ drug - weight\ of\ free\ drug)}{Weight\ of\ initial\ drug} \times 100$$

2.6.2 Percent drug content

Each formulation's 1gm weight was put into a 50 mL volumetric flask with 50 mL of water, and the mixture was agitated for 30 minutes. The volume was filtered and made up to 50 mL. Once more, 1 mL of the a forementioned solution was diluted to a final concentration of 10 mL

Using alcohol after being previously diluted to 1 mL. A spectrophotometric analysis of the solution's absorbance was performed [22]. From four batches batch – NP-3 showed maximum drug content hence subjected to further evaluations.

2.6.3 Scanning electron microscope (SEM)

Prepare the TFG nanoparticle sample by dispersing it onto a suitable substrate, such as a carbon-coated grid. Ensured the sample was dry and free from contamination. Opened the JEOL JSM6360 Scanning microscope chamber and evacuated it to achieve a vacuum. Adjusted the working distance and electron beam parameters (e.g., accelerating voltage) suitable for the sample. The sample was grounded and properly mounted on the stage. Aligned the beam to the desired area of the sample surface using the optical microscope built into the SEM. Imaging parameters were set, such as magnification and scan speed, for obtaining high-resolution images. After that the imaging process was done by scanning the electron beam across the sample surface. Analyzed the obtained SEM images photograph of formulation's particle size to study the surface morphology of TFG NPs. Measured the particle sizes, shapes, and surface roughness using the provided software. Digital images of TFG NPs complex were captured by random scanning of the stub at 1000, 5000, 10000, and 30000 X magnifications [23].

2.6.4 Fourier transform – infra red spectroscopy (FT-IR)

Simply by comparing the spectrums of the complex, its individual components, and mechanical mixes, FTIR can corroborate the spectroscopic assessment of the generated complex. Pellets were created by combining samples 1:100 with dry, crystalline KBr. Before being compressed into KBr disc, the mixture was crushed or triturated into a fine powder using an agate mortar. At a resolution of 2, each KBr disc was scanned at a rate of 4 mm/s. Another useful method for validating the stability of the NPs complex is FTIR [24].

2.6.5 Differential scanning calorimetry (DSC)

The thermal stress of the excipients' medicinal ingredients and their interactions throughout the formulation process are assessed using thermodynamical approaches. The thermal analysis of TFG NPs, were placed in an aluminum crimp cell and heated at a rate of 100°C/min from 0 to 400°C in a nitrogen atmosphere (TA Instruments, USA, model DSC Q10 V24.4 Build 116). Using an analyzer, the peak transition onset temperatures were recorded. In an aluminum crimp cell (TA Instruments, USA, Model DSC Q10 V24.4 Build 116), TFG leaves extract were added. The cell was heated at 100°C/min from 0 to 400°C in a nitrogen environment. Using an analyzer, the peak transition onset temperatures were recorded [25].

Journal of Chemical Health Risks

www.jchr.org

JCHR (2024) 14(4), 544-560 | ISSN:2251-6727

2.6.6 Particle size and zeta potential(PS & ZP)

ZP and PS of TFG NPs were measured by dynamic light scattering (DLS) using a Malvern Zetasizer Nano-ZS (Malvern Instruments, Worcestershire, UK). At a 173° angle, scattered light was noticed. The material was diluted before each measurement, and the temperature was maintained at 25 °C throughout to confirm the results. The equipment we employed also systematically and automatically adjusts to the sample, the laser's intensity, and the attenuator. As a result, it is guaranteed that the experimental measurement circumstances can be replicated [26].

2.6.7 Transmission electron microscopy (TEM)

The NPs morphology was visually examined using a JEOL JEM 1400 (Japan) Transmission Electron Microscopy (TEM). Before the sample was analyzed, a total of 10 mL of sample was disseminated. A drop of the sample was then applied to the specimen after the mixture had been mixed. The specimens were covered with a 400-mesh grid, which was left in place for a minute. A filter paper was used to remove any remaining droplets from the grid. The grid was covered with a drop of uranyl acetate, and the remaining surplus solution was filtered out using filter paper. After 30 minutes on the grid, the films were inspected under a transmission electron microscope [27].

2.6.8 X-ray diffraction (XRD)

When appropriately interpreted and contrasted with the drug's pre-formulation XRD pattern, the XRD is a unique technique for determining a compound's crystallinity and allows the detection of drug crystalline changes. The material's crystallinity was assessed using XRD on pure extract and NPs. A PHILIPS XPert Pro X-Ray Diffractometer was used to scan the sample in the angular range of 50 to 800. A dried sample that was kept in a sample container (20 mm 15 mm 2 mm) that was introduced into the apparatus was examined using an X-ray [28-30].

3. Results and Discussion

3.1. Collection of plant material

The initial phase of this study involved the meticulous collection of Trigonella Foenum-Graceum, widely recognized as fenugreek, from the expansive botanical garden at MUP's College of Pharmacy in Risod. The selection of this plant species was deliberate, considering its extensively documented pharmacological properties and rich historical usage. The botanical garden, known for its controlled and consistent cultivation conditions, served as an optimal environment for the systematic collection, guaranteeing the reliability and uniformity of the acquired specimens.

3.2. Authentication

Subsequent to the collection, a stringent authentication process was undertaken to validate the precision of the obtained Trigonella Foenum-Graceum plant material. This process encompassed the comprehensive documentation of essential botanical characteristics, growth conditions, and other pertinent metadata. Additionally, botanical experts were engaged to visually scrutinize and confirm the identity of the specimens, relying on distinctive features such as leaf morphology and flower structure.

Furthermore, voucher specimens of the collected plant materials were systematically submitted to the herbarium, creating a tangible repository for future reference and cross-verification. This authentication procedure not only upholds rigorous scientific standards but also assures the subsequent analyses are based on authentic Trigonella Foenum-Graceum material, thereby establishing a solid foundation for reliable and credible research.

3.33. Organoleptic evaluation

Organoleptic evaluation refers to the evaluation of the material to be justified by color, odor, taste etc. The TFG extractives exhibited organoleptic characteristics in the following ways: the nature appeared as a coarse powder, the color presented a dull green, the odor was distinctly bitter, and the taste was characterized by a pronounced bitterness as given in the Table 2**.**

Table 2: Organoleptic evaluation of TFG

Sr.no.	Parameter	Observation
1	Nature	Coarse powder
2	Color	Dull green
3	Odor	Bitter
4	Taste	Bitter

Journal of Chemical Health Risks

www.jchr.org

JCHR (2024) 14(4), 544-560 | ISSN:2251-6727

3.4. Microscopical evaluation

The anatomical section of TFG, commonly known as fenugreek, revealed the presence of both upper and lower epidermis. Upon peeling the leaf's epidermal layer, Anisocytic stomata with trichomes were observed. Anisocytic stomata are characterized by their irregular shape and orientation, with one large subsidiary cell accompanied by two smaller subsidiary cells was showed in Figure 7.1. Trichomes, on the other hand, there was hair-like structures that can be found on the leaf surface. This anatomical arrangement is significant for fenugreek's role in regulating transpiration and protecting against external factors**.**

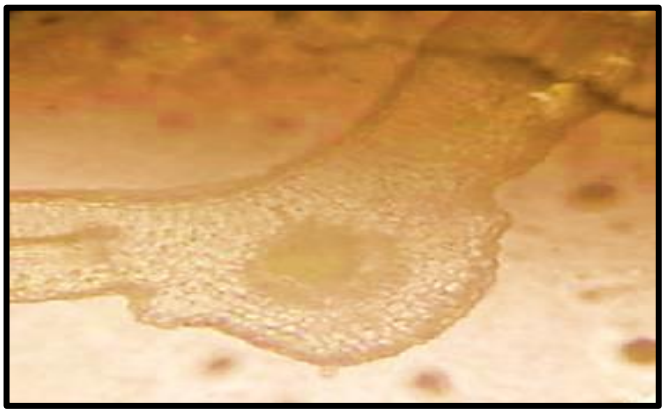

Figure 1: Microscopical evaluation of TFG

3.5. Physicochemical evaluation

The physicochemical analysis of the research samples produced significant findings. Ash values were calculated for determining the materials' inorganic composition, loss on drying was measured to evaluate their moisture content, and extractive values were computed to estimate their solubility. These variables offer essential details regarding the quality and purity of the substances under investigation, assisting in the characterization and standardization of the materials. The obtained data of overall study explore in Table 3.

Table 3: Physicochemical evaluation of TFG

Sr.no.	Parameter	Observation
1	**Loss on drying**	3.57± 0.12
2	**Determination of Ash values**	
	i)Total ash content	5.36± 0.13
	ii)Acid Insoluble Ash	1.17±0.1
	iii)Water Soluble Ash	2.14±0.11
	iv)Sulphated ash	3.15±0.18
3	**Determination of extractive values**	
	i) Water soluble extractive	14.29±0.04
	ii) Alcohol soluble extractive	9.82±0.17

Journal of Chemical Health Risks

www.jchr.org

JCHR (2024) 14(4), 544-560 | ISSN:2251-6727

3.6. Phytochemical studies for following

During the analysis, different phytoconstituents including alkaloids, phenolic compounds and tannins, flavonoids, carbohydrates, and sugars were identified. This comprehensive identification process aids in the isolation of the active metabolites. The Table no.7.3 revealed that the extract exhibited higher levels of alkaloids, steroids, carbohydrates, and tannins compared to other constituents.

Table 4: Identification of Phytoconstituent

(+) =Test positive (presence of constituent) (-) = Test negative (Absent)

Constituent	Pet Ether	Chloroform	Ethyl Acetate	Methanol	Aqueous
Alkaloid	+	+	+	+	+
Glycoside	-	-	-	-	-
Steroid	+	-	-	+	+
Carbohydrate	-	-	-	+	+
Protein	-	-	-	-	-
Amino Acid	-	-	-	-	-
Tannin	-	-	+	+	+
Saponin	-	-	-	-	-
Mucilage	-	-	-	-	-

3.7 Extraction of TFG leaves

Extraction of TFG leaves was done by Soxhlet extraction method using ethanol. A preliminary phytochemical investigation of extract discussed in subsequent section.

3.7.1 Thin layer chromatography (TLC)

Distances travelled by both the solute (the material being analyzed) and the solvent (the liquid used to convey the solute) are significant parameters in TLC. The Retention Factor (RF) value is the proportion of the solute's and solvent's respective travel distances. It is a dimensionless quantity that helps in the identification and categorization of the mixture's constituents.

Therefore, the calculated RF value was approximately 0.4583, which suggests that the solute was more strongly attracted to the stationary phase (the solid or liquid material on the TLC plate) than to the mobile phase (the solvent) which is showed in Figure 2.

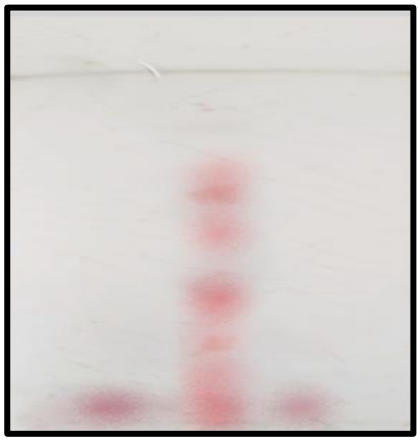

Figure 2: Thin Layer chromatography of TFG extract

Journal of Chemical Health Risks

www.jchr.org

JCHR (2024) 14(4), 544-560 | ISSN:2251-6727

3.7.2 High-performance thin layer chromatography (HPTLC)

The HPTLC fingerprint studied for methanol extract of TGF was performed. The plate was produced in a Camag twin TLC chamber with an 8 cm-high cover using Pet ether: Acetone (8:2) as the mobile phase. The plate was derivatized by being submerged in anisaldehyde H2SO4. Scanner 3 scanned the plate at a wavelength of 274 nm. 3 bands of TGF observed in the HPTLC fingerprint plate at 0.65,0.68 and 0.66 Rf values, as shown figure 3,4 and 5. The highest Rf value of the compound was found to be 0.68.

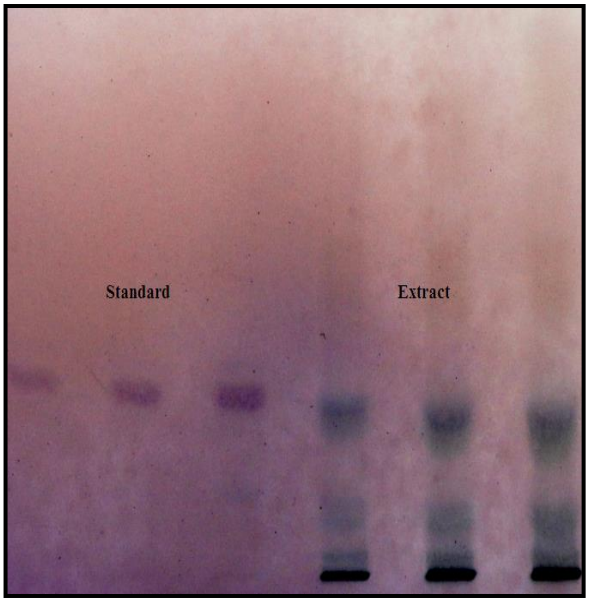

Figure 3: HPTLC fingerprinting of standard TGF and TGF extract.

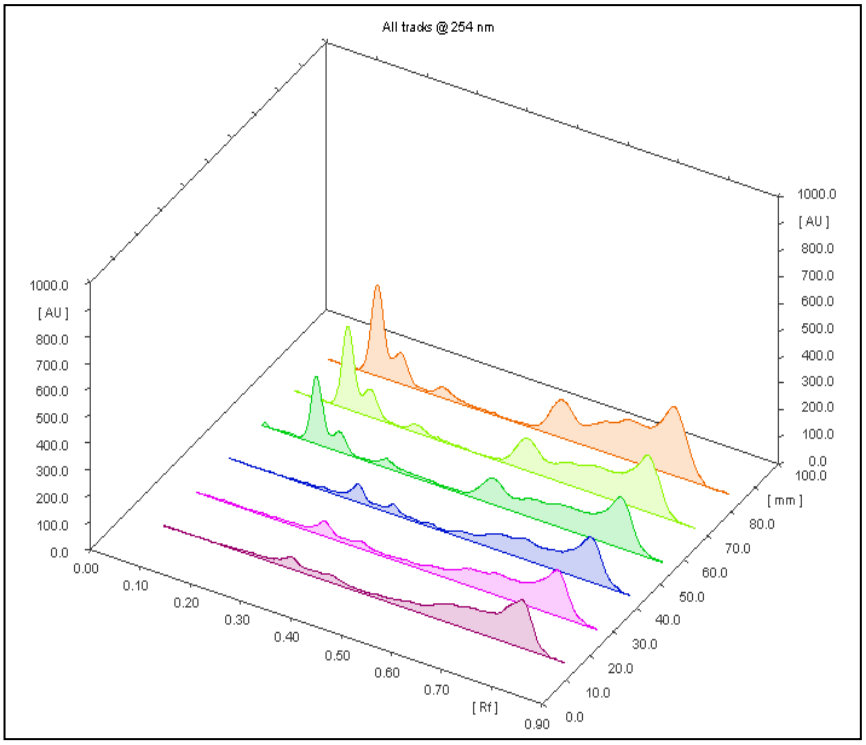

Figure 4: HPTLC chromatogram of standard TGF and TGF extract.

Journal of Chemical Health Risks

www.jchr.org

JCHR (2024) 14(4), 544-560 | ISSN:2251-6727

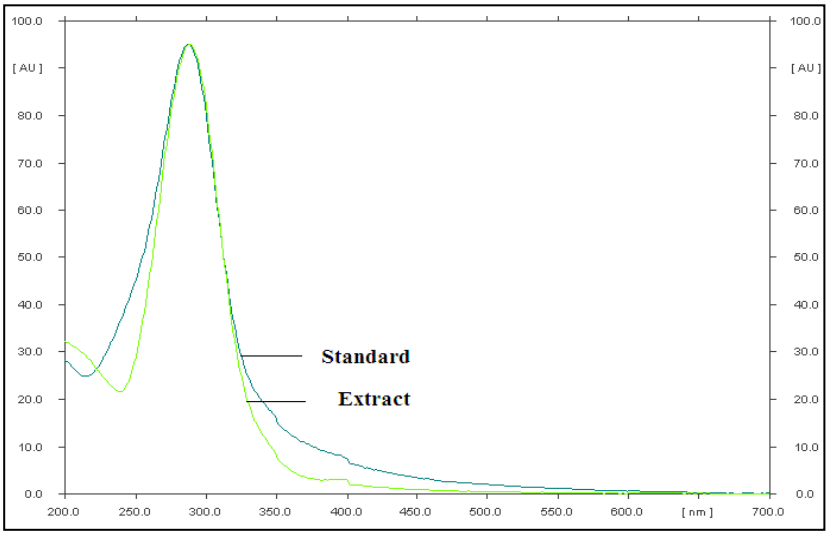

Figure 5: Overlay of standard TGF and TGF extract.

3.8 Development of formulation

The development of nanoparticle formulations using the lyophilization (freeze-drying) method was carried out using a benchtop freeze dryer. Four different formulations with varying concentrations of chitosan and extract were prepared with 20mL methanol as given in Table 5. Lyophilization involved the process of freezing the nanoparticle suspensions and then subjecting them to vacuum conditions, causing the frozen water to sublime directly from ice to vapor, resulting in the formation of dry nanoparticles. This technique is beneficial for enhancing the stability and shelf-life of the nanoparticles, as well as facilitating their reconstitution upon rehydration. The study aimed to optimize the formulation parameters and chitosan concentrations to achieve desired nanoparticle characteristics for potential applications

Table 5: Different NPs with different molar ratio of chitosan and extract with methanol

Nanoparticles batch	Molar ratio Chitosan(mg): extract(mg)	Methanol
NP-1	0.5:1	20 mL
NP-2	1:1	20 mL
NP-3	2:1.5	20 mL
NP-4	3:2	20 mL

3.9 Evaluation of NPS

Entrapment efficiency:

TFG nanoparticles formulations prepared with a 2:1.5 ratio of Chitosan: Extract (2.0%) shown in Table 5 showed higher entrapment efficiency irrespective of the type of surfactant. This might be because raising the surfactant concentration causes the drug's solubility in lipids to increase.

Percent drug content:

The nanoparticle formulation NP-3 demonstrated the highest drug content among all the nanoparticles studied, indicating that NP3 had the most efficient drug loading. As well as the nanoparticles formulation with same molar ratio of Chitosan and Extract i.e., NP-3 showed great percent drug content which is given in Figure 6.

Journal of Chemical Health Risks

www.jchr.org

JCHR (2024) 14(4), 544-560 | ISSN:2251-6727

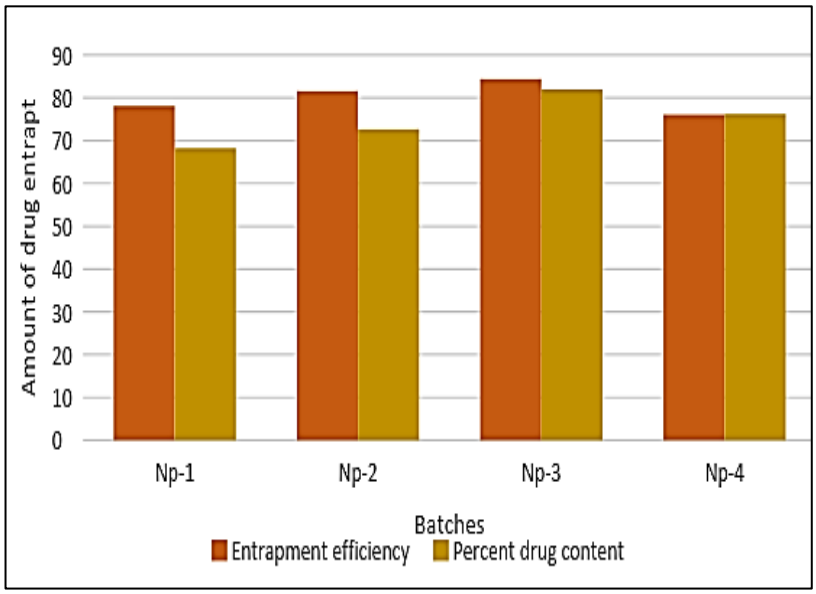

Figure 6: Bar graph showing both Entrapment efficiency and

Scanning electron microscopy (SEM)

The SEM images displayed 2um-sized nanoparticles with irregular shapes. The photographs revealed smooth-surfaced, irregularly shaped as shown in Figure 7. Agglomeration was observed, potentially influencing dispersibility and overall nanoparticle activity.

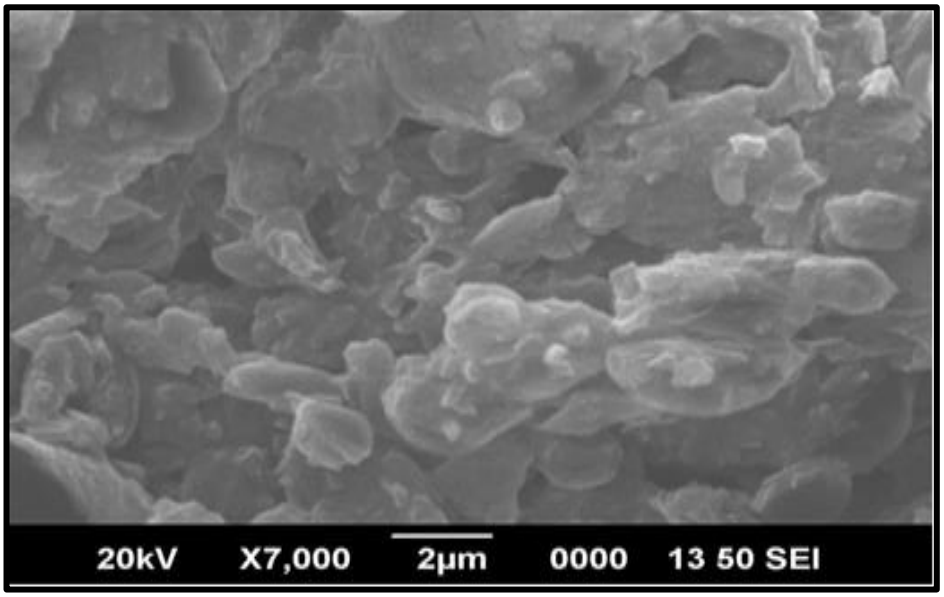

Figure 7: Scanning electron microscope image of TFG NPs

Fourier transform – infra red spectroscopy (FT-IR)

Figure 8 displays the FTIR spectra of the drug and the drug with excipients. The presence of similar functional groups such as C-H aromatic stretching, C-H aliphatic stretching, C=O stretching, C=C aromatic stretching, and C-CL aromatic stretching at 3134, 2968, 1699, 1512, and 1043 cm-1, respectively, in the initial FTIR spectrum of the drug polymer mixture, supported the compatibility of the drug with the excipients.

Journal of Chemical Health Risks

www.jchr.org

JCHR (2024) 14(4), 544-560 | ISSN:2251-6727

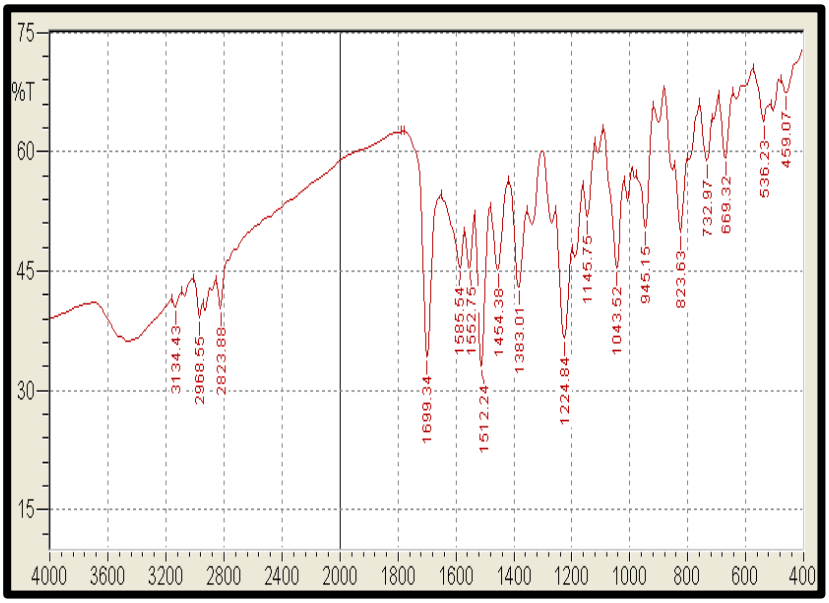

Figure 8: FTIR Spectrum of TFG NPs of NP-3

Differential scanning calorimetry (DSC):

The DSC observation for the nanoparticles NP-3 revealed that they underwent a melting process at a temperature of 208.47°C. During the DSC analysis, the sample was subjected to controlled heating or cooling while measuring the heat flow associated with its thermal transitions. In this case, the observed melting point of 208.47°C in Figure 9 indicates the temperature at which the nanoparticles transitioned from a solid state to a liquid state. The melting point is a characteristic property of a substance and provides insights into its purity, crystallinity, and thermal stability.

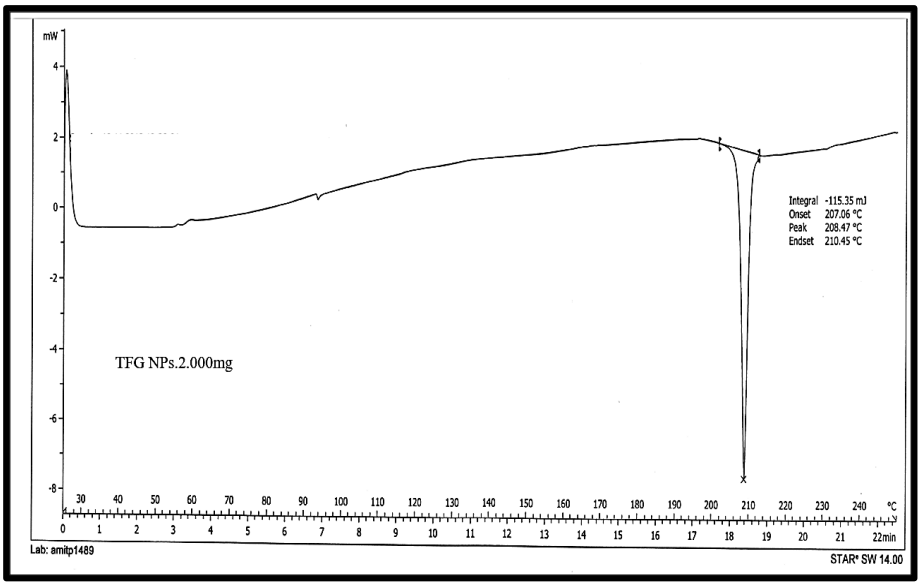

Figure 9: Differential scanning calorimetry for TFG NP3

Particle size and zeta potential (PS & ZP):

ZP is one of the fundamental characteristics that is known to have an impact on stability. It measures the strength of the electrostatic or charge repulsion or attraction between particles. It was discovered that greater ZP results in less particle aggregation because of electric repulsion and therefore greater nanoparticle stability, and vice versa. According to Figures 7.10 and 7.11, the ZP value for batch NP3 was -26.5 and the PS for NP-3 was discovered to be 131.1.

Journal of Chemical Health Risks

www.jchr.org

JCHR (2024) 14(4), 544-560 | ISSN:2251-6727

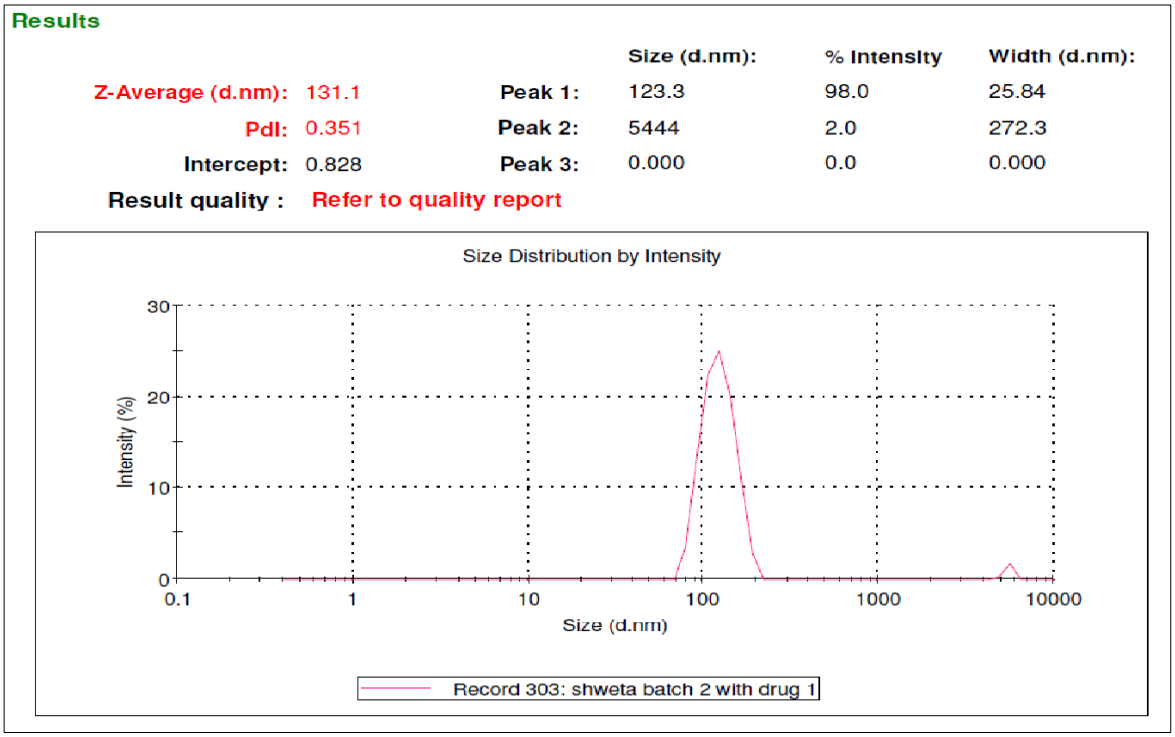

Figure 10: Particle size of NPs-3.

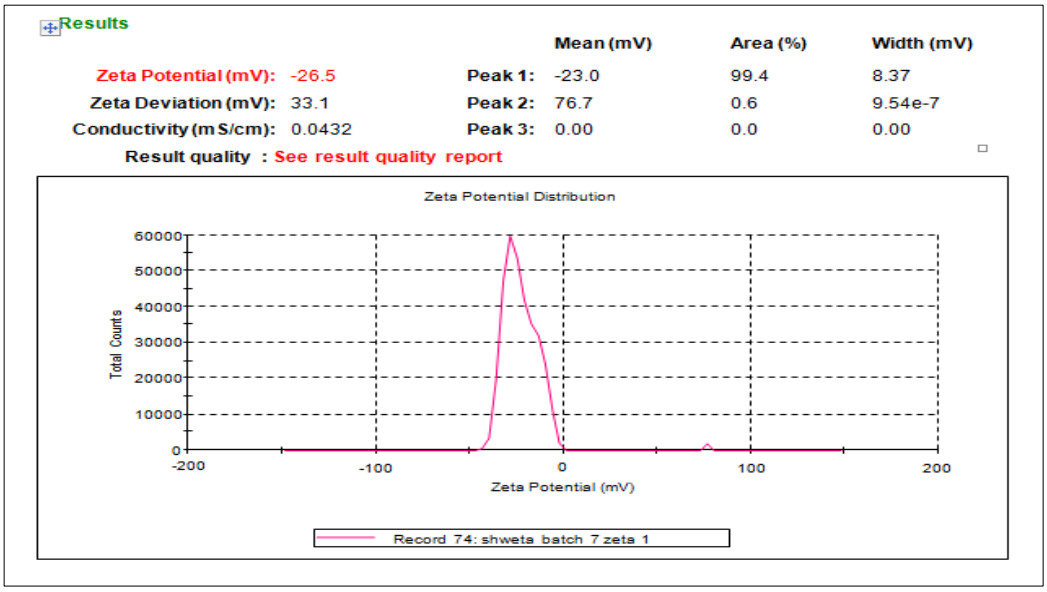

Figure 11: Zeta potential of NPs-3

Transmission Electron Microscopy (TEM):

The TEM images of TFG-NP3 nanoparticles reveal their uniform distribution, smooth texture, and spherical shape, as evident in Figure 12. This characterization underscores their controlled synthesis, crucial for reproducibility. Smooth surfaces enhance interactions with materials, while spherical morphology influences stability and cellular interactions. These findings highlight their potential for applications in drug delivery, biomedical imaging, and material science.

Journal of Chemical Health Risks
www.jchr.org
JCHR (2024) 14(4), 544-560 | ISSN:2251-6727

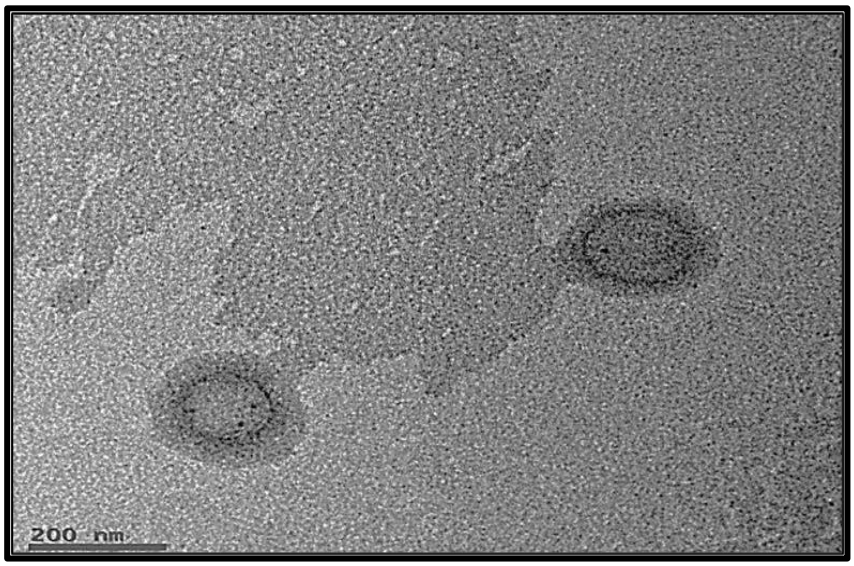

Figure 12: TEM image of TFG NPs

X-ray diffraction (XRD):

X-ray powder diffraction studies have been most valuable in evaluation of phase behavior, arrangement, and crystal order of molecule. The X-ray diffractogram NP-3 showed sharp peak at different angles (2Ɵ) 5.896, 13.521, 18.061, 19.511, 22.215 and 23.255 showing a typical crystalline pattern as given in Figure 13.

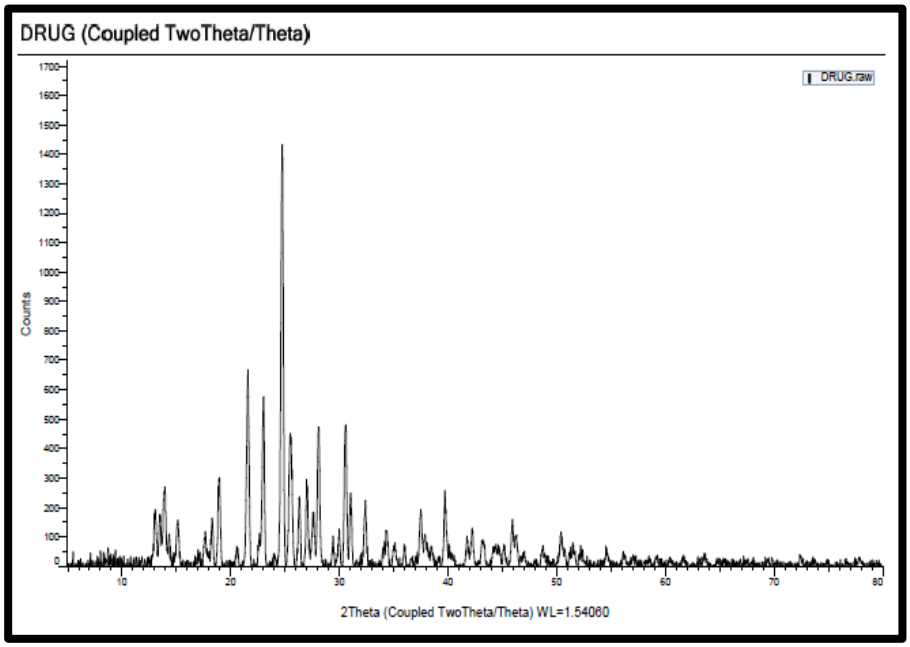

Figure 13: X-ray Diffractogram of TFG NPs

4. Conclusion

In conclusion, this research aimed to develop a natural nanoparticle (NP) formulation for diabetes treatment based on Trigonella foenum-graceum (fenugreek). By employing lipid-based drug delivery strategies and nanotechnology principles, the study effectively addressed formulation challenges, enhancing the solubility, bioavailability, and therapeutic efficacy of fenugreek. Through systematic optimization utilizing statistical tools and experimental design techniques, the formulated NPs exhibited desirable attributes such as ideal particle size, high drug loading, and physical stability. Characterization results demonstrated that these lipid-based fenugreek NPs outperformed traditional formulations, potentially improving medication

absorption and solubility. Although animal model studies underscored their enhanced bioavailability and therapeutic efficacy, further investigations encompassing pharmacokinetic and pharmacodynamic assessments are warranted to elucidate their clinical relevance.

In summary, the successful development, formulation, and optimization of lipid-based fenugreek NPs for diabetes treatment presented in this thesis offer valuable insights into pharmaceutical sciences. This discovery underscores the potential of NPs as efficacious drug delivery vehicles, opening avenues for enhancing the effectiveness of poorly soluble natural compounds like fenugreek in diabetes management. Future research endeavors should focus on comprehensive in vitro and in vivo evaluations to elucidate the pharmacological mechanisms and clinical applicability of these innovative formulations, advancing the frontier of diabetes therapeutics.

Acknowledgment

The authors would like to express their sincere gratitude to the Department of Pharmacy, Sunrise University, Alwar, for providing the necessary facilities and support for conducting this research. We are thankful for the guidance and encouragement received from the faculty members, whose expertise and insights have greatly contributed to the successful completion of this study. Additionally, we extend our appreciation to the university administration for fostering an environment conducive to academic and research endeavors. This work was made possible through the collaborative efforts and dedication of all individuals associated with the Department of Pharmacy at Sunrise University, Alwar.

Conflict of interest

The authors declare no conflict of interest regarding the publication of this research article manuscript.

Refrences

1. Tao Z, Shi A, Zhao J. Epidemiological Perspectives of Diabetes. Cell Biochem Biophys [Internet]. 2015 Sep 25;73(1):181–5. Available from: http://link.springer.com/10.1007/s12013-015-0598-4
2. Eid S, Sas KM, Abcouwer SF, Feldman EL, Gardner TW, Pennathur S, et al. New insights into the mechanisms of diabetic complications: role of lipids and lipid metabolism. Diabetologia [Internet]. 2019 Sep 25;62(9):1539–49. Available from: http://link.springer.com/10.1007/s00125-019-4959-1
3. Dal Canto E, Ceriello A, Rydén L, Ferrini M, Hansen TB, Schnell O, et al. Diabetes as a cardiovascular risk factor: An overview of global trends of macro and micro vascular complications. Aboyans V, Cosentino F, editors. Eur J Prev Cardiol [Internet]. 2019 Dec 1;26(2_suppl):25–32. Available from: https://academic.oup.com/eurjpc/article/26/2_suppl/25/5925419
4. Cerf ME. Beta Cell Dysfunction and Insulin Resistance. Front Endocrinol (Lausanne) [Internet]. 2013;4. Available from: http://journal.frontiersin.org/article/10.3389/fendo.2013.00037/abstract
5. Roep BO, Thomaidou S, van Tienhoven R, Zaldumbide A. Type 1 diabetes mellitus as a disease of the β-cell (do not blame the immune system?). Nat Rev Endocrinol [Internet]. 2021 Mar 8;17(3):150–61. Available from: https://www.nature.com/articles/s41574-020-00443-4
6. Holt RIG, DeVries JH, Hess-Fischl A, Hirsch IB, Kirkman MS, Klupa T, et al. The management of type 1 diabetes in adults. A consensus report by the American Diabetes Association (ADA) and the European Association for the Study of Diabetes (EASD). Diabetologia [Internet]. 2021 Dec 30;64(12):2609–52. Available from: https://link.springer.com/10.1007/s00125-021-05568-3
7. Banday MZ, Sameer AS, Nissar S. Pathophysiology of diabetes: An overview. Avicenna J Med [Internet]. 2020 Oct 4;10(04):174–88. Available from: http://www.thieme-connect.de/DOI/DOI?10.4103/ajm.ajm_53_20
8. Khawandanah J. Double or hybrid diabetes: A systematic review on disease prevalence, characteristics and risk factors. Nutr Diabetes [Internet]. 2019 Nov 4;9(1):33. Available from: https://www.nature.com/articles/s41387-019-0101-1
9. Yang B, Li J, Haller MJ, Schatz DA, Rong L. The progression of secondary diabetes: A review of modeling studies. Front Endocrinol (Lausanne) [Internet]. 2022 Dec 21;13. Available from: https://www.frontiersin.org/articles/10.3389/fendo.2022.1070979/full
10. McIntyre HD, Catalano P, Zhang C, Desoye G, Mathiesen ER, Damm P. Gestational diabetes mellitus. Nat Rev Dis Prim [Internet]. 2019 Jul 11;5(1):47. Available from: https://www.nature.com/articles/s41572-019-0098-8

11. Harrison's Online. Diabetes Mellitus > Insulin Biosynthesis, Secretion, and Action. In: Endocrinology and Metabolism. p. Section 1.
12. Bonnefond A, Unnikrishnan R, Doria A, Vaxillaire M, Kulkarni RN, Mohan V, et al. Monogenic diabetes. Nat Rev Dis Prim [Internet]. 2023 Mar 9;9(1):12. Available from: https://www.nature.com/articles/s41572-023-00421-w
13. Wild SH, Byrne CD. Risk factors for diabetes and coronary heart disease. BMJ [Internet]. 2006 Nov 11;333(7576):1009–11. Available from: https://www.bmj.com/lookup/doi/10.1136/bmj.39024.568738.43
14. Daryabor G, Atashzar MR, Kabelitz D, Meri S, Kalantar K. The Effects of Type 2 Diabetes Mellitus on Organ Metabolism and the Immune System. Front Immunol [Internet]. 2020 Jul 22;11. Available from: https://www.frontiersin.org/article/10.3389/fimmu.2020.01582/full
15. Nauck MA, Wefers J, Meier JJ. Treatment of type 2 diabetes: challenges, hopes, and anticipated successes. Lancet Diabetes Endocrinol [Internet]. 2021 Aug;9(8):525–44. Available from: https://linkinghub.elsevier.com/retrieve/pii/S2213858721001133
16. Martín-Peláez S, Fito M, Castaner O. Mediterranean Diet Effects on Type 2 Diabetes Prevention, Disease Progression, and Related Mechanisms. A Review. Nutrients [Internet]. 2020 Jul 27;12(8):2236. Available from: https://www.mdpi.com/2072-6643/12/8/2236
17. Padhi S, Nayak AK, Behera A. Type II diabetes mellitus: a review on recent drug based therapeutics. Biomed Pharmacother [Internet]. 2020 Nov;131:110708. Available from: https://linkinghub.elsevier.com/retrieve/pii/S0753322203090 1X
18. Pleus S, Freckmann G, Schauer S, Heinemann L, Ziegler R, Ji L, et al. Self-Monitoring of Blood Glucose as an Integral Part in the Management of People with Type 2 Diabetes Mellitus. Diabetes Ther [Internet]. 2022 May 13;13(5):829–46. Available from: https://link.springer.com/10.1007/s13300-022-01254-8
19. Alsayed Hassan D, Curtis A, Kerver J, Vangsnes E. Diabetes Self-Management Education and Support: Referral and Attendance at a Patient-Centered Medical Home. J Prim Care Community Health [Internet]. 2020 Jan 29;11:215013272096723. Available from: http://journals.sagepub.com/doi/10.1177/2150132720967232
20. Salmerón-Manzano E, Garrido-Cardenas JA, Manzano-Agugliaro F. Worldwide Research Trends on Medicinal Plants. Int J Environ Res Public Health [Internet]. 2020 May 12;17(10):3376. Available from: https://www.mdpi.com/1660-4601/17/10/3376
21. Li X, Wu L, Wu R, Sun M, Fu K, Kuang T, et al. Comparison of medicinal preparations of Ayurveda in India and five traditional medicines in China. J Ethnopharmacol [Internet]. 2022 Feb;284:114775. Available from: https://linkinghub.elsevier.com/retrieve/pii/S0378874121010059
22. Roy A, Khan A, Ahmad I, Alghamdi S, Rajab BS, Babalghith AO, et al. Flavonoids a Bioactive Compound from Medicinal Plants and Its Therapeutic Applications. Ullah R, editor. Biomed Res Int [Internet]. 2022 Jun 6;2022:1–9. Available from: https://www.hindawi.com/journals/bmri/2022/5445291/
23. Usai R, Majoni S, Rwere F. Natural products for the treatment and management of diabetes mellitus in Zimbabwe-a review. Front Pharmacol [Internet]. 2022 Aug 24;13. Available from: https://www.frontiersin.org/articles/10.3389/fphar.2022.980819/full
24. Heba M. A, Ayman A. M. Medicinal plants and their validation challenges in traditional Egyptian medicine. J Appl Pharm Sci [Internet]. 2022 Mar 5; Available from: https://www.japsonline.com/abstract.php?article_id=3582&sts=2
25. Atanasov AG, Zotchev SB, Dirsch VM, Supuran CT. Natural products in drug discovery: advances and opportunities. Nat Rev Drug Discov [Internet]. 2021 Mar 28;20(3):200–16. Available from: https://www.nature.com/articles/s41573-020-00114-z
26. Salehi, Ata, V. Anil Kumar, Sharopov, Ramírez-Alarcón, Ruiz-Ortega, et al. Antidiabetic Potential of Medicinal Plants and Their Active Components. Biomolecules [Internet]. 2019 Sep 30;9(10):551. Available from: https://www.mdpi.com/2218-273X/9/10/551
27. Tewabe A, Abate A, Tamrie M, Seyfu A, Abdela Siraj E. Targeted Drug Delivery — From Magic Bullet to Nanomedicine: Principles, Challenges, and Future

Perspectives. J Multidiscip Healthc [Internet]. 2021 Jul;Volume 14:1711–24. Available from: https://www.dovepress.com/targeted-drug-delivery--from-magic-bullet-to-nanomedicine-principles-c-peer-reviewed-fulltext-article-JMDH

28. Mitchell MJ, Billingsley MM, Haley RM, Wechsler ME, Peppas NA, Langer R. Engineering precision nanoparticles for drug delivery. Nat Rev Drug Discov [Internet]. 2021 Feb 4;20(2):101–24. Available from: https://www.nature.com/articles/s41573-020-0090-8
29. Harish V, Ansari MM, Tewari D, Gaur M, Yadav AB, García-Betancourt ML, et al. Nanoparticle and Nanostructure Synthesis and Controlled Growth Methods. Nanomaterials [Internet]. 2022 Sep 16;12(18):3226. Available from: https://www.mdpi.com/2079-4991/12/18/3226
30. Patra JK, Shin HS, Das G. Characterization and Evaluation of Multiple Biological Activities of Silver Nanoparticles Fabricated from Dragon Tongue Bean Outer Peel Extract. Int J Nanomedicine [Internet]. 2021 Feb;Volume 16:977–87. Available from: https://www.dovepress.com/characterization-and-evaluation-of-multiple-biological-activities-of-s-peer-reviewed-article-IJN